



# Hard processes in small systems

Dennis V. Perepelitsa<sup>a</sup>

<sup>a</sup>*University of Colorado Boulder, 390 UCB, Boulder, CO 80309*

---

## Abstract

These proceedings from the Quark Matter 2017 conference give an overview of the latest experimental results on hard processes in small collision systems at RHIC and the LHC, discuss their implications, and consider several prospects for future measurements.

*Keywords:*

---

## 1. Introduction

These proceedings give an overview of high transverse momentum ( $p_T$ ) jet, hadron and electroweak probes of small (e.g. proton–nucleus or  $p+A$ ) collision systems. They are organized around three components of such a collision: the initial state of the nucleus, the initial state of the proton, and the final state of the system. I emphasize results which are new since the previous Quark Matter conference, attempt to place them into context with other experimental data and theoretical ideas, and suggest avenues for future work.

## 2. Initial state of the nuclear wavefunction

Measurements of the inclusive production of jets and charged particles, the most abundant QCD final-state objects, are a fundamental way to characterize the partonic content of, and fragmentation process in, a hadronic collision system. Some measurements of these signatures in 5.02 TeV  $p+Pb$  collision data recorded in early 2013 at the LHC initially suggested that charged particle production rates at large  $p_T$  and the jet-to-particle fragmentation function may be modified to a surprisingly large degree with respect to proton–proton ( $pp$ ) collisions. However, these measurements lacked directly measured  $pp$  comparison data at the same energy and thus generally relied on extrapolated references with large uncertainties.

At this conference, an updated set of experimental results were presented which use a directly-measured 5.02 TeV  $pp$  reference from the high-luminosity data recorded in late 2015 at the LHC. Two important examples are shown in Fig. 1. Measurements of charged particle production rates from ATLAS [1] and CMS [2] indicate that they exhibit only a modest enhancement in the anti-shadowing region,  $p_T \approx 40 - 80$  GeV and are otherwise consistent at lower  $p_T$  with the initial measurement by ALICE [3]. The enhancement at large hadron- $p_T$  is qualitatively similar to that observed in the ATLAS measurement of inclusive jet production [4]. Additionally, an updated measurement of jet fragmentation functions from ATLAS [5] showed that they are consistent with those in  $pp$  data, now agreeing with a preliminary CMS measurement [6]. Thus, the

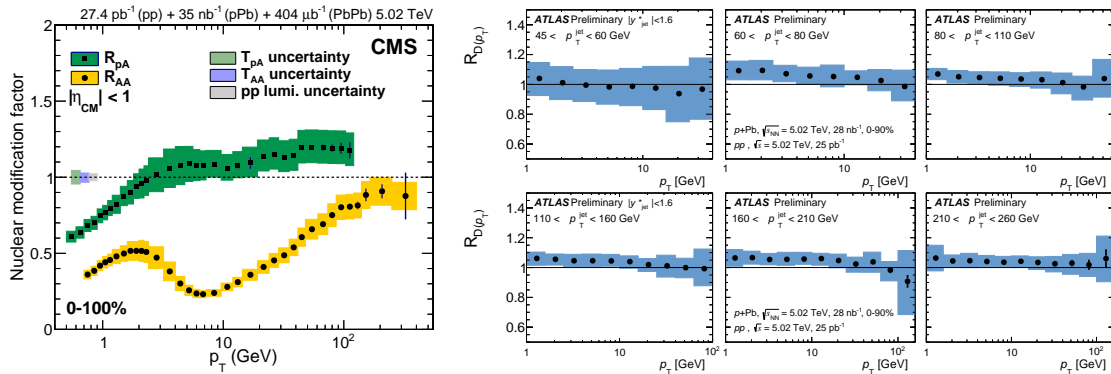


Fig. 1. Measurements of the nuclear modification factor for charged particles (left, from CMS [2]) and jet-to-particle fragmentation function (right, from ATLAS [5]) in 5.02 TeV  $p+Pb$  collisions, each using a directly measured 5.02 TeV  $pp$  reference.

latest available data on inclusive charged hadron production, jet production, and jet-to-hadron fragmentation together give a mutually consistent picture of the basic QCD hard scattering process in  $p+A$  collisions.

The inclusion of 5.02 TeV  $pp$  reference data has also brought clarity to the interpretation of measurements in other channels. For example, it has eliminated the theoretical uncertainties in previous measurements by ATLAS of how  $Z$  boson production rates are modified in  $p+Pb$  collisions, demonstrating that they are consistent with expectations from analyses of parton distribution functions in nuclei (nPDFs) [7]. On the other hand, the inclusion of  $pp$  data in measurements of dijet production by CMS has revealed that current nuclear PDF sets are insufficient to describe modifications in certain kinematic regions [8]. A particular disagreement is found in the so called EMC region (large nuclear- $x \gtrsim 0.2$ ) at large- $Q^2$ . Measurements in this kinematic region are particularly important for giving context to new results presented at this conference by ATLAS on the suppression of TeV-scale jets in Pb+Pb collisions [9]: the  $p+Pb$  measurements constrain how much of the observed suppression in Pb+Pb may be expected from initial state, rather than final state, effects. In any case, the improved dijet and electroweak boson data are now being used in the next generation of global nPDF extractions such as the EPPS16 analysis in Ref. [10].

### 2.1. Photo-nuclear processes and precision electroweak probes

Despite the breadth of these measurements, it is useful to further improve the accessible kinematic range and experimental precision of measured initial state effects. One promising possibility is the use of hard photo-nuclear processes in ultra-peripheral nucleus-nucleus collisions [11] (i.e. those with an impact parameter much larger than the nuclear radii). Schematically, a quasi-real photon emitted by one nucleus may split into a quark-antiquark dipole and scatter with a gluon in the other nucleus, generically resulting in dijet production. These collisions can be distinguished from ordinary low-multiplicity inelastic (peripheral) Pb+Pb collisions through their event topology, which features large pseudorapidity gaps in particle production on one side of the detector. Thus these processes allow for measurements of nuclear effects on jet production without the substantial experimental complications introduced by the high-multiplicity underlying event present in hadronic nuclear collisions, allowing jets to be measured at low  $p_T$  values. In this conference, ATLAS presented a preliminary measurement of photo-nuclear dijet production cross-sections over an expansive kinematic range [12] (Fig. 2, left). In particular, this measurement is sensitive to nuclear PDF effects in a  $(x_A, Q^2)$  range normally inaccessible in existing fixed-target deep inelastic scattering data and the LHC dijet and electroweak data described above. When published in a fully unfolded form, this measurement has the potential to provide a large input to nPDF analyses in regions not directly constrained by any data. The CMS and ALICE experiments presented new results on the photoproduction of heavy vector mesons in ultra-peripheral Pb+Pb collisions [13, 14], providing complementary data at lower  $Q^2$ .

The 8.16 TeV  $p+Pb$  data recently collected at the LHC in late 2016 also offers new opportunities for further precision studies of the initial nuclear state. In particular, the substantially larger luminosity of

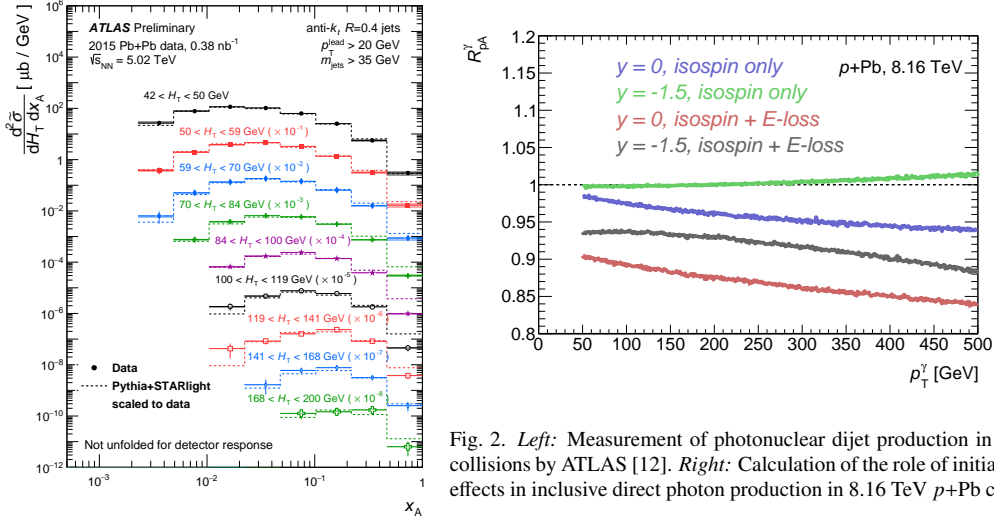


Fig. 2. *Left*: Measurement of photonuclear dijet production in 5.02 TeV Pb+Pb collisions by ATLAS [12]. *Right*: Calculation of the role of initial state energy loss effects in inclusive direct photon production in 8.16 TeV  $p$ +Pb collisions [16, 17].

this dataset compared to the lower-energy  $p$ +Pb data collected in 2013 ( $170 \text{ nb}^{-1}$  vs.  $31 \text{ nb}^{-1}$ ) as well as the modestly larger cross-sections for hard-scattering processes will enable high-statistics measurements in electroweak channels. Unlike the situation at the time of the 5.02 TeV  $p$ +Pb data-taking, precision measurements of QCD and electroweak processes in the existing high-statistics 8 TeV  $pp$  data collected in 2012 can be used as the reference for 8.16 TeV  $p$ +Pb collisions (with only a modest correction for the small collision energy difference). To give one example of the quality of the readily available reference data, the systematic uncertainty in existing measurements of the photon production cross-section in 8 TeV  $pp$  collisions [15] reaches  $\sim 2\%$  for 80–300 GeV photons at mid-rapidity, including luminosity uncertainties.

I give three specific examples of electroweak measurements enabled by this large-luminosity dataset: (1) Inclusive direct photon production rates can be measured at central and forward rapidities out to several hundred GeV, where calculations suggest they will be sensitive to non-trivial initial state energy loss effects [16, 17] (Fig. 2, right). (2) Di-photon production can be measured for the first time in a heavy ion context. This fundamental QCD process is sensitive, through a box diagram with internal quark loop, to the gluon distribution in both beams, allowing for experimentally clean access to the low nuclear- $x$  regime. (The scientific motivation is similar as in Ref. [18] but with a kinematic region closer to that previously measured in the LHC as in Ref. [19].) (3) Top quarks can be observed for the first time in heavy ion collisions, for example through  $t\bar{t}$  production in which both top quarks produce a high- $p_T$  electron or muon in their decay chain. Such a measurement would be sensitive to nuclear modifications of the gluon PDF at large nuclear- $x$ , a kinematic region which is otherwise difficult to access experimentally [20].

## 2.2. Measurements as a function of centrality

In addition to measurements in minimum bias (inclusive in event-activity)  $p$ +A collisions, the centrality- or event-activity-dependence of hard process rates in small collision systems is interesting. Such measurements are traditionally motivated as a way to probe the impact parameter dependence of nPDF modification or, for example, the nuclear thickness dependence of initial state energy loss effects. More generally, they test the combined understanding of soft and hard particle production processes in these collision systems.

In  $p$ +A collisions, the first attempts to measure centrality-selected hard process rates have generally found that they are inconsistent with the binary-collision-scaled expectation from  $pp$  collisions. Frequently, these observations are discussed as arising from a “bias”, for example, in the event selection or estimation of geometric parameters. In fact, there are at least two distinct effects, with distinct physics origins, signs, and kinematic dependences. The first effect is the conventional *centrality bias*, most visible at moderate- $p_T$  values ( $\lesssim 10 \text{ GeV}$  or  $\lesssim 50 \text{ GeV}$  at RHIC and LHC energies, respectively), which causes a kinematics-independent increase (decrease) of the yield in central (peripheral) collisions. This effect arises because the

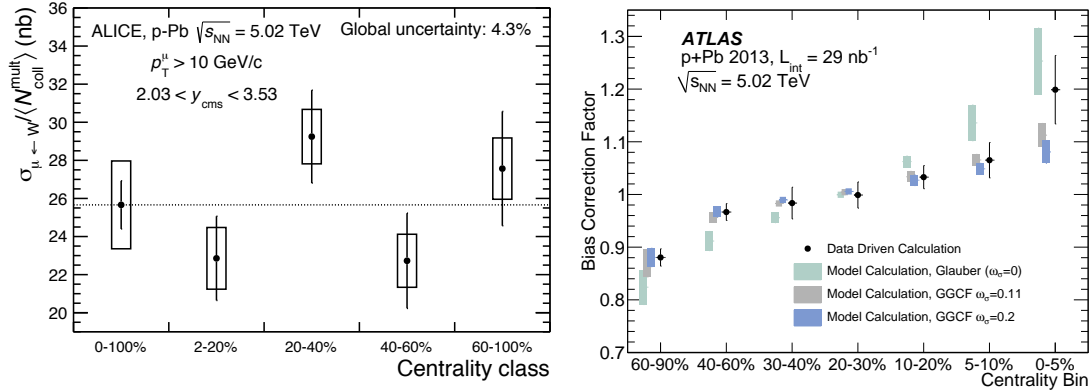


Fig. 3. *Left*: ALICE measurement of the centrality-dependence of  $W^\pm$  production in 5.02 TeV  $p$ +Pb collisions [22] within the hybrid model [21]. *Right*: Calculation of centrality bias factors with data-driven [25] and analytic [23] methods for  $p$ +Pb collisions in ATLAS.

increased multiplicity associated with the presence of a hard parton–parton scattering causes hard-scatter  $p$ +A events to be categorized in a higher-activity centrality class than the centrality calibration, derived from analyzing minimum-bias events without a hard scatter, would predict.

The experiments have found several methods to correct for or eliminate this first bias. I summarize them here: (1) In the “hybrid method” developed by ALICE,  $p$ +Pb events are categorized by their energy signature in the zero-degree calorimeter far downstream of the Pb nucleus [21], which has a large pseudorapidity separation from the mid-rapidity region. Since the distribution of energies in this kinematic region is difficult to associate to a Glauber model, the geometric parameters are estimated by assuming that they scale with the soft particle multiplicity elsewhere in the event. Using this method, ALICE has presented a new measurement of  $W^\pm$  production which demonstrates a binary-collision scaling [22] (Fig. 3, left). (2) One may calculate the quantitative effects of the bias on measured yields based on the correlation between hard process rates and underlying event activity in  $pp$  collisions, such as the method used by ATLAS [23] which builds on previous work in this vein by PHENIX [24] (Fig. 3, right). When applied to  $p$ +Pb collision data, these corrections generally restore the expected binary collision scaling for electroweak boson and quarkonia production, as shown by ATLAS [25]. (3) Third, one may argue that the bias arises from an incomplete modeling of  $p$ +A collision geometries. In particular, event-to-event color fluctuations in the configuration of the proton, which in the context of geometric modeling is implemented in the so-called Glauber-Gribov Color Fluctuation (GGCF) model [26, 27], may play an important role. In fact, some measurements, such as that of femtoscopic radii in centrality-selected  $p$ +Pb collisions presented by ATLAS at this conference [28], suggest a preference for the broader  $N_{\text{part}}$  distribution in the GGCF model over that in the traditional Glauber model. When geometric parameters are estimated under the GGCF model, hard-process yields (such as  $Z$  bosons in Ref. [25]) are closer to the  $pp$ -based expectation before any additional corrections.

The second “bias” is a physics effect which for mid-rapidity processes is relevant only at large  $p_T$  ( $> 10$  GeV and  $\gtrsim 200$  GeV at RHIC and the LHC, respectively). Although it may manifest as a bias in observables such as nuclear modification factors, it has a distinctive experimental signature from the conventional centrality bias described above. Here I briefly describe the essential features observed in data: (1) Rates of high- $p_T$  jet production at mid-rapidity at RHIC are observed to be “split” in centrality: they are suppressed (enhanced) in central (peripheral) collisions, in a way that grows with increasing jet- $p_T$ , but in such a way that they integrate to a null effect for minimum bias collisions [29]. (2) Rates of high- $p_T$  jet production at the LHC are modified in an analogous way at a much larger jet- $p_T$  range but, when measuring at mid-rapidity, in a similar  $x_T = 2p_T/\sqrt{s}$  range,  $x_T \gtrsim 0.1$  [4]. (3) At systematically more proton-going rapidities, the centrality-splitting effect is evident at systematically smaller jet- $p_T$  values and nuclear modification factors scale with  $p_T \cosh(y) \sim E_{\text{jet}}$  across six units of rapidity. In a leading order picture, jets with total energy

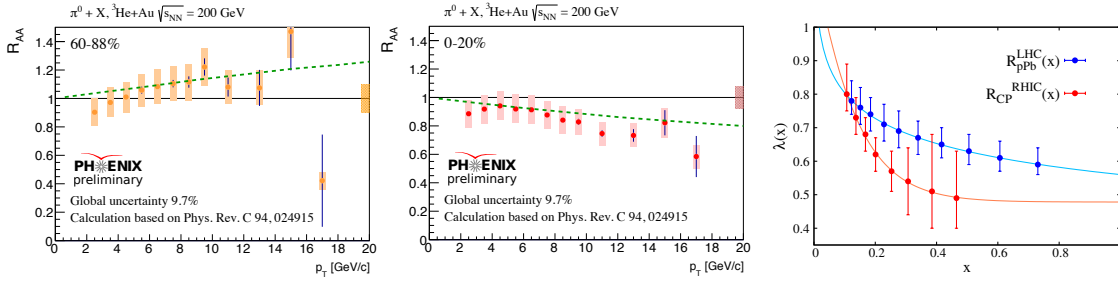


Fig. 4. *Left and center*: Measurement by PHENIX of the “centrality splitting” in high- $p_T$   $\pi^0$  production in  ${}^3\text{He}+\text{Au}$  collisions [38] compared to the calculation in Ref. [37]. *Right*: Extracted values of  $\lambda(x_p)$ , the ratio of the interaction cross-section for nucleons in a large- $x_p$  configuration to that for average configurations, at RHIC (red) and LHC (blue) energies [40].

$E_{\text{jet}}$  in the forward region are most commonly produced from parton–parton configurations with Bjorken- $x_p$  in the proton given by  $x_p \approx 2E_{\text{jet}}/\sqrt{s}$  (as noted for example in Ref. [30]). (4) Measurements of the pseudorapidity distributions for dijet pairs shows that their production at forward rapidities is systematically suppressed (enhanced) with selections on large (small) event activity [31]. (5) Finally, a control analysis of how transverse energy production at large (one-sided) rapidity broadly depends on parton–parton scattering kinematics [32] refutes the suggestion that this effect is caused by a rapidity-separated “energy conservation”, extending a similar conclusion reached by studying hard processes at mid-rapidity in Ref. [24].

Together, the collision-energy- and rapidity-dependence of the centrality-splitting effect in data strongly suggests that it is controlled predominantly by only one kinematic variable: the Bjorken- $x_p$  of the hard-scattered parton in the proton beam or, perhaps, Feynman- $x_F = x_p - x_A$  which is numerically similar to  $x_p$  in the forward region. As will be described below, this observation suggests that the data is sensitive to an  $x_p$ -dependent property of the proton wavefunction before the collision. However, an initial state energy loss effect which depends predominantly on  $x_F$  [33] may also play some role.

### 3. Initial state of the proton wavefunction

One efficient explanation of the observed centrality-dependence of hard process rates at large  $x_p > 0.1$  is that it arises from a change in the properties of protons with a large- $x_p$  parton. This and similar ideas are developed in Refs. [30, 34, 35, 36]. Schematically, the *shrinking proton* picture supposes that protons in a large- $x_p$  configuration have a smaller transverse size, fewer additional partons, and interact with other nucleons with a smaller cross-section, than average protons. When protons in a large- $x_p$  configuration pass through the nucleus, they interact with fewer nucleons than a proton in an average configuration would, and therefore a smaller centrality signature is produced in the collision than is expected given its underlying geometric configuration. Thus production rates in minimum bias (e.g. centrality-averaged) collisions are unmodified, but events with a large- $x_p$  proton are systematically redistributed to a more peripheral classification. Since the size or interaction strength of the proton decreases with increasing  $x_p$ , this provides an efficient explanation for the observed set of data at multiple rapidities and collision energies.

I list several ways in which the shrinking proton picture can be further tested experimentally or additional ways in which aspects of this physics can be explored: (1) A unique test may be performed with the recently collected 200 GeV  $p+\text{Au}$  and  ${}^3\text{He}+\text{Au}$  collision data recorded at RHIC. The centrality-splitting effect is expected to be larger in the  $p+\text{Au}$  system relative to that in the  $d+\text{Au}$  system since the absence of a (non-shrinking) nucleon in the projectile beam will strengthen the relative effect, and vice versa for the  ${}^3\text{He}+\text{Au}$  system [37]. Preliminary data presented by PHENIX on  $\pi^0$  production in  ${}^3\text{He}+\text{Au}$  collisions [38] follows this expected projectile-species dependence (Fig. 4, left). An analogous set of preliminary  $p+\text{Au}$  data observes a large central-to-peripheral difference as expected, but this difference modulates an overall suppression across all centrality selections (including minimum-bias collisions), suggesting some impact from the  $pp$  reference common to each  $p+\text{Au}$  centrality selection which should be further explored. (2)

In addition to the overall transverse size of the beam-remnant, the momentum and spatial structure of the remainder of the proton in a large- $x_p$  configuration could be studied. One experimental prospect enabled by the high-luminosity  $p$ +Pb data is the study of so-called double-parton scattering events, in which two distinct partons in the proton participate in independent hard-scatterings with partons in the nucleus [39]. Schematically, after first requiring evidence of a large- $x_p$  scattering, one could explore the how the kinematics of the second, independent hard-scattering are correlated with event activity. (3) The RHIC and the LHC data could be analyzed within a consistent theoretical framework to extract how the proton size shrinks with  $x_p$  at different collision energies. Such an analysis is sensitive to how the cross-section for small-proton configurations grows with energy relative to that for average configurations (with the preliminary result of such an extraction [40] shown in Fig. 4, right). (4) Measurements of the centrality-dependence of other (for example, electroweak) processes at large- $x_p$  can test whether the shrinking of the proton depends on the flavor of the parton, and otherwise confirm that the shrinking of the proton in the initial state is process-independent.

#### 4. Final state effects in small systems

In addition to the initial state physics motivations described above, hard processes may also be used to test for the final-state energy loss of partons traversing a small-sized region of dense colored matter or quark-gluon plasma which, as is recently suggested by experimental signatures in the soft sector, may be created in these collision systems. At this conference, new results were presented on the suppression of inclusive jet and hadron spectra in peripheral nucleus–nucleus (A+A) collisions, which also feature a small nuclear overlap. For example, a new measurement of the hadron  $R_{AA}$  by CMS reveals that is suppressed by 30% in 70–90% Pb+Pb collisions (Fig. 5, left). Pb+Pb events in this centrality range include eleven participating nucleons on average, only slightly more than the average number in  $p$ +Pb collisions. Furthermore, a simple comparison of the transverse geometry of very peripheral A+A and central  $p$ +A collisions in a Glauber or state-of-the-art hydrodynamic model [41] reveals that they are not as different as one may (naively) expect. While there are plausible reasons that  $p$ +A collisions may behave differently than A+A collisions with a similar transverse geometric extent, the absence of obvious jet quenching signatures in  $p$ +A collisions is notable given the large suppression easily observed in even very glancing A+A collisions.

Given the complications in interpreting the centrality-selected hard process measurements described above (some trivial, some due to non-trivial but ultimately unrelated large- $x$  physics), parton energy loss effects may instead be probed event-by-event through intra-event momentum correlations which are expected to be modified in the presence of energy loss. One example is the azimuthal anisotropy  $v_2$  of high- $p_T$  charged particles in high-activity events. In fact, a previous measurement by ATLAS observed that the rapidity-separated azimuthal correlation function for  $p_T = 10$  GeV particles exhibits a visible near-side peak, with  $v_2 \approx 0.05$ , in the most central 1% of 5.02 TeV  $p$ +Pb events [42]. In A+A collisions, this signature would be traditionally interpreted as a path-length-dependent modification in particle production resulting from final-state energy loss. Another example is the  $p_T$  balance between high- $p_T$  final state objects, which does not rely on an unbiased estimate of geometric quantities. At this conference, a preliminary measurement of the  $p_T$  spectrum of high- $p_T$  hadron-triggered recoil jets was presented by ALICE [43], concluding that is is unmodified in 0–20% central  $p$ +Pb collisions relative to that in peripheral collisions (Fig. 5, right), placing a limit on the possible amount of energy loss. Considered together, the two results provoke the question of whether an onset of jet quenching may be observed at some centrality interval between these two.

To resolve any potential tension between peripheral A+A and central  $p$ +A data, I suggest efforts along three lines: (1) The experimental selection and modeling of very peripheral A+A collisions, frequently overlooked due to the low hard process yield and small overlap region, should be re-examined. Uncertainties on geometric parameters are significant in the most peripheral A+A collisions ( $> 15\%$  in the CMS  $R_{AA}$  measurement [2]), largely driven by the uncertainty in the fraction of inelastic A+A collisions selected by triggers. Although current measurements of the  $N_{coll}$ -scaling of electroweak bosons in Pb+Pb collisions [44] offers some confirmation of the geometric picture, they are statistically limited in peripheral collisions. A fresh look, using the improved understanding of contaminating EM processes and pseudorapidity-gap based event classification, would be welcome. (2) Jet quenching calculations or Monte Carlo models which correctly describe the full centrality-dependence of jet quenching signatures in A+A collisions should be

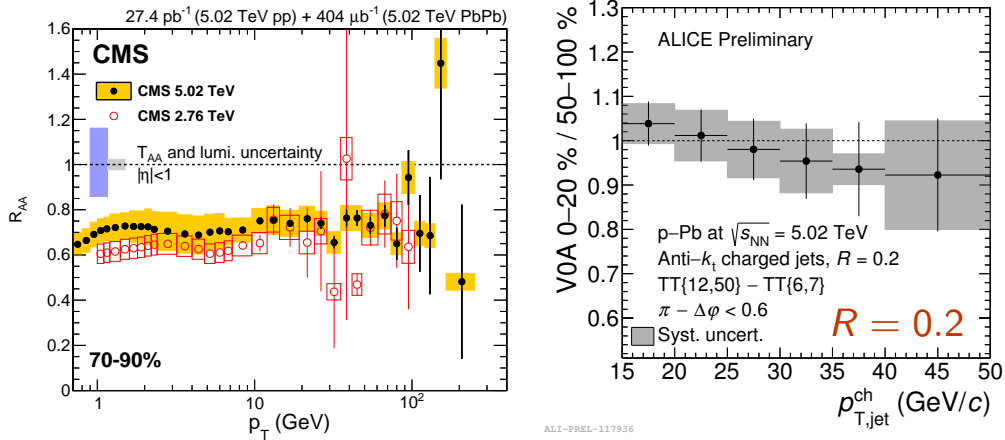


Fig. 5. Left: CMS measurement of the  $R_{AA}$  for charged particles in 70–90% central ( $\langle N_{\text{part}} \rangle \approx 11$ ) 5.02 TeV Pb+Pb collisions [2]. Right: ALICE measurement of the hadron-triggered recoil jet  $p_T$  spectrum, ratio of 0–20%  $p$ +Pb events to that in 50–100% events [43].

challenged to simultaneously describe the available data in very peripheral A+A and central  $p$ +A collisions. (3) Finally, the signatures above can be explored in more detail in the high-luminosity 8.16 TeV  $p$ +Pb data. Using high-multiplicity triggers enabled during data-taking, experiments can extend measurements of two-particle correlations to higher  $p_T$  and a wider centrality range. The data will also provide ample statistics for jet+X  $p_T$ -correlations: for example, results on photon–jet correlations presented at this conference [45, 46] demonstrate that they can be measured with good systematic control in  $pp$  events. Based on existing measurements of isolated photon production cross-sections in 8 TeV  $pp$  collisions [15], it is expected that the 8.16 TeV  $p$ +Pb data contains more than ten thousand photons with  $p_T^\gamma > 40$  GeV in the 1% highest-multiplicity events, allowing for a high-statistics, well-controlled search for energy loss effects.

Such questions could also be explored through collisions of intermediate-sized nuclei. For example, a program of Ar+Ar collisions at the LHC would achieve a large luminosity with a level of underlying event activity amenable to precision measurements of energy loss signatures even for low- $p_T$  jets.

## 5. Conclusion

These proceedings discuss new results on hard processes in small systems presented at the Quark Matter conference, focusing on the insight they provide into the initial state of the nuclear and proton wavefunctions and into any final state effects in the resulting system. For each topic, I have attempted to suggest directions for future measurements or analysis, which I hope will be available in time for the next Quark Matter.

## References

- [1] ATLAS Collaboration, Measurement of charged particle spectra in  $pp$  collisions and nuclear modification factor  $R_{pPb}$  at  $\sqrt{s_{NN}} = 5.02$  TeV with the ATLAS detector at the LHC, ATLAS-CONF-2016-108.
- [2] V. Khachatryan, et al., Charged-particle nuclear modification factors in PbPb and pPb collisions at  $\sqrt{s_{NN}} = 5.02$  TeV, JHEP 04 (2017) 039.
- [3] B. B. Abelev, et al., Transverse momentum dependence of inclusive primary charged-particle production in p-Pb collisions at  $\sqrt{s_{NN}} = 5.02$  TeV, Eur. Phys. J. C74 (2014) 3054.
- [4] G. Aad, et al., Centrality and rapidity dependence of inclusive jet production in  $\sqrt{s_{NN}} = 5.02$  TeV proton-lead collisions with the ATLAS detector, Phys. Lett. B748 (2015) 392–413.
- [5] ATLAS Collaboration, Measurement of jet fragmentation in 5.02 TeV proton-lead and proton-proton collisions with the ATLAS detector, ATLAS-CONF-2017-004.
- [6] CMS Collaboration, Jet Fragmentation Function in pPb Collisions at  $\sqrt{s_{NN}} = 5.02$  TeV and  $pp$  Collisions at  $\sqrt{s} = 2.76$  and 7 TeV, CMS-PAS-HIN-15-004.

- [7] ATLAS Collaboration, Z Boson Production in pp Collisions at  $\sqrt{s} = 5.02$  TeV with the ATLAS detector at the LHC, ATLAS-CONF-2016-107.
- [8] CMS Collaboration, Dijet pseudorapidity in pp and pPb collisions at  $\sqrt{s_{NN}} = 5.02$  TeV with the CMS detector, CMS-PAS-HIN-16-003.
- [9] ATLAS Collaboration, Study of inclusive jet yields in Pb+Pb collisions at  $\sqrt{s_{NN}} = 5.02$  TeV, ATLAS-CONF-2017-009.
- [10] K. J. Eskola, P. Paakkinen, H. Paukkunen, C. A. Salgado, EPPS16: Nuclear parton distributions with LHC data, Eur. Phys. J. C77 (2017) 163.
- [11] M. Strikman, R. Vogt, S. N. White, Probing small x parton densities in ultraperipheral AA and pA collisions at the LHC, Phys. Rev. Lett. 96 (2006) 082001.
- [12] ATLAS Collaboration, Photo-nuclear dijet production in ultra-peripheral Pb+Pb collisions, ATLAS-CONF-2017-011.
- [13] E. Kryshen, et al., Photoproduction of heavy vector mesons in ultra-peripheral Pb-Pb collisions, *ibid.*
- [14] D. T. Takaki, et al., Evidence of nuclear gluon effects in  $\gamma$ +Pb interactions, *ibid.*
- [15] G. Aad, et al., Measurement of the inclusive isolated prompt photon cross section in pp collisions at  $\sqrt{s} = 8$  TeV with the ATLAS detector, JHEP 08 (2016) 005.
- [16] Y.-T. Chien, et al., Jet Quenching from QCD Evolution, Phys. Rev. D93 (2016) 074030.
- [17] I. Vitev, B.-W. Zhang, A Systematic study of direct photon production in heavy ion collisions, Phys. Lett. B669 (2008) 337–344.
- [18] A. Kovner, A. H. Rezaeian, Diphoton ridge in p+p and p+A collisions at RHIC and the LHC, Phys. Rev. D92 (2015) 074045.
- [19] G. Aad, et al., Measurement of the isolated di-photon cross-section in pp collisions at  $\sqrt{s} = 7$  TeV with the ATLAS detector, Phys. Rev. D85 (2012) 012003.
- [20] D. d’Enterria, K. Krajczar, H. Paukkunen, Top-quark production in proton-nucleus and nucleus-nucleus collisions at LHC energies and beyond, Phys. Lett. B746 (2015) 64–72.
- [21] J. Adam, et al., Centrality dependence of particle production in p-Pb collisions at  $\sqrt{s_{NN}} = 5.02$  TeV, Phys. Rev. C91 (2015) 064905.
- [22] J. Adam, et al., W and Z boson production in p-Pb collisions at  $\sqrt{s_{NN}} = 5.02$  TeV, JHEP 02 (2017) 077.
- [23] D. V. Perepelitsa, P. A. Steinberg, Calculation of centrality bias factors in p+A collisions based on a positive correlation of hard process yields with underlying event activity, arXiv:1412.0976.
- [24] A. Adare, et al., Centrality categorization for  $R_{p(d)+A}$  in high-energy collisions, Phys. Rev. C90 (2014) 034902.
- [25] G. Aad, et al., Z boson production in p+Pb collisions at  $\sqrt{s_{NN}} = 5.02$  TeV measured with the ATLAS detector, Phys. Rev. C92 (2015) 044915.
- [26] G. Aad, et al., Measurement of the centrality dependence of the charged-particle pseudorapidity distribution in proton-lead collisions at  $\sqrt{s_{NN}} = 5.02$  TeV with the ATLAS detector, Eur. Phys. J. C76 (2016) 199.
- [27] M. Alvioli, M. Strikman, Color fluctuation effects in proton-nucleus collisions, Phys. Lett. B722 (2013) 347–354.
- [28] M. Aaboud, et al., Femtoscopy with identified charged pions in proton-lead collisions at  $\sqrt{s_{NN}} = 5.02$  TeV with ATLAS, arXiv:1704.01621.
- [29] A. Adare, et al., Centrality-dependent modification of jet-production rates in deuteron-gold collisions at  $\sqrt{s_{NN}} = 200$  GeV, Phys. Rev. Lett. 116 (2016) 122301.
- [30] M. Alvioli, B. A. Cole, L. Frankfurt, D. V. Perepelitsa, M. Strikman, Evidence for x-dependent proton color fluctuations in pA collisions at the CERN Large Hadron Collider, Phys. Rev. C93 (2016) 011902.
- [31] S. Chatrchyan, et al., Studies of dijet transverse momentum balance and pseudorapidity distributions in pPb collisions at  $\sqrt{s_{NN}} = 5.02$  TeV, Eur. Phys. J. C74 (2014) 2951.
- [32] G. Aad, et al., Measurement of the dependence of transverse energy production at large pseudorapidity on the hard-scattering kinematics of proton-proton collisions at  $\sqrt{s} = 2.76$  TeV with ATLAS, Phys. Lett. B756 (2016) 10–28.
- [33] Z.-B. Kang, I. Vitev, H. Xing, Effects of cold nuclear matter energy loss on inclusive jet production in p+A collisions at energies available at the BNL Relativistic Heavy Ion Collider and the CERN Large Hadron Collider, Phys. Rev. C92 (2015) 054911.
- [34] A. Bzdak, V. Skokov, S. Bathe, Centrality dependence of high energy jets in p+Pb collisions at energies available at the CERN Large Hadron Collider, Phys. Rev. C93 (2016) 044901.
- [35] N. Armesto, D. Gulhan, G. Milhano, Kinematic bias on centrality selection of jet events in pPb collisions at the LHC, Phys. Lett. B747 (2015) 441–445.
- [36] M. Kordell, A. Majumder, Jets in d(p)-A Collisions: Color Transparency or Energy Conservation, arXiv:1601.02595.
- [37] D. McGlinchey, J. L. Nagle, D. V. Perepelitsa, Consequences of high-x proton size fluctuations in small collision systems at  $\sqrt{s_{NN}} = 200$  GeV, Phys. Rev. C94 (2016) 024915.
- [38] D. McGlinchey, et al., PHENIX Overview, *ibid.*
- [39] B. Blok, M. Strikman, U. A. Wiedemann, Hard four-jet production in pA collisions, Eur. Phys. J. C73 (2013) 2433.
- [40] M. Alvioli, L. Frankfurt, D. V. Perepelitsa, M. Strikman, *in preparation.*
- [41] R. D. Weller, P. Romatschke, One fluid to rule them all: viscous hydrodynamic description of event-by-event central p+p, p+Pb and Pb+Pb collisions at  $\sqrt{s} = 5.02$  TeV, arXiv:1701.07145.
- [42] G. Aad, et al., Measurement of long-range pseudorapidity correlations and azimuthal harmonics in  $\sqrt{s_{NN}} = 5.02$  TeV proton-lead collisions with the ATLAS detector, Phys. Rev. C90 (2014) 044906.
- [43] A. Timmins, et al., ALICE Overview, *ibid.*
- [44] ATLAS Collaboration, Z boson production in Pb+Pb collisions at  $\sqrt{s_{NN}} = 5.02$  TeV with the ATLAS detector at the LHC, ATLAS-CONF-2017-010.
- [45] ATLAS Collaboration, Study of photon-jet momentum correlations in Pb+Pb and pp collisions at  $\sqrt{s_{NN}} = 5.02$  TeV with ATLAS, ATLAS-CONF-2016-110.
- [46] CMS Collaboration, Study of Isolated photon jet correlation in PbPb and pp collisions at 2.76 TeV and pPb collisions at 5.02 TeV, CMS-PAS-HIN-13-006.